Functional Immobilization and Patterning of Proteins by an Enzymatic Transfer Reaction

ARTICLE *in* ANALYTICAL CHEMISTRY · FEBRUARY 2010

Impact Factor: 5.64 · DOI: 10.1021/ac902608a · Source: PubMed

7 AUTHORS, INCLUDING:

Maniraj Bhagawati
University of California, Berkeley
13 PUBLICATIONS **152** CITATIONS
SEE PROFILE

Yulia Podoplelova
Universität Osnabrück
5 PUBLICATIONS **218** CITATIONS
SEE PROFILE

Jacob Piehler
Universität Osnabrück
158 PUBLICATIONS **4,951** CITATIONS
SEE PROFILE

Anal. Chem. **2010,** *82,* 1478–1485

Functional Immobilization and Patterning of Proteins by an Enzymatic Transfer Reaction

Sharon Waichman, Maniraj Bhagawati, Yulia Podoplelova, Annett Reichel, Ariane Brunk, Dirk Paterok, and Jacob Piehler*

Division of Biophysics, University of Osnabrück, Barbarastrasse 11, 49076 Osnabrück, Germany

Functional immobilization and lateral organization of proteins into micro- and nanopatterns is an important prerequisite for miniaturizing bioanalytical and biotechnological devices. Here, we report an approach for efficient site-specific protein immobilization based on enzymatic phosphopantetheinyl transfer (PPT) from coenzyme A (CoA)-functionalized glass-type surfaces to specific peptide tags. We devised a bottom-up surface modification approach for coupling CoA densely to a molecular poly(ethylene glycol) polymer brush. Site-specific enzymatic immobilization of proteins fused to different target peptides for the PPTase Sfp was confirmed by real-time label-free detection. Quantitative protein−protein interaction experiments confirmed that significantly more than 50% of the immobilized protein was fully active. The method was successfully applied with different proteins. However, different immobilization efficiencies of PPT-based immobilization were observed for different peptide tags being fused to the N- and C-termini of proteins. On the basis of this immobilization method, we established photolithographic patterning of proteins into functional binary microstructures.

Protein immobilization on solid supports is rapidly gaining importance not only for analytical applications such as functional proteomics,[1] medical diagnostics, and drug screening,[2,3] but also for the construction of biomedical and bioanalytical devices[4] and for fundamental biophysical research.[5] These applications require targeting of proteins into microscopic and nanoscopic structures, while preserving their functional integrity to the highest possible level. Functional attachment of proteins to solid supports is a key challenge because of the fragile nature of proteins and their wide-ranging physicochemical properties. For this purpose, protein capturing techniques are required, which site-specifically tether proteins to biocompatible polymer layers through protein or peptide tags fused to the protein of interest. However, selective recognition pairs with high binding stability are required for successful application in surface engineering. Recognition units for efficient capturing of proteins to surfaces, which are compatible with surface patterning, are scarce. Several approaches based on either the interaction between biotin and streptavidin or related proteins,[6−9] or on the complexation of immobilized transition metal ions by oligohistidine-tags[10−14] have been reported. Multiplexed surface biofunctionalization, however, requires orthogonal, generic approaches for functional protein immobilization. Next to chemical approaches such as chemical ligation,[15] Staudinger ligation,[16] thiol−ene reaction,[8] or "Click chemistry" utilizing azide alkyne Huisgen cycloaddition,[17] enzymatic reactions have found increasing attention for posttranslational labeling and immobilization of proteins.[18,19] Surface chemistries based on protein fusion to engineered enzymes,[20] which specifically react with immobilized substrate analogues, have been developed.[21,22] Recently, a versatile approach for site-specific protein modification was reported, which is based on enzymatic phosphopantetheinyl transfer (PPT) from coenzyme A (CoA) derivatives to a serine residue of peptidyl[23,24] or acyl carrier proteins.[25] These reactions

* To whom correspondence should be addressed. E-mail: piehler@uos.de.

(1) Zhou, H.; Roy, S.; Schulman, H.; Natan, M. J. *Trends Biotechnol.* **2001**, *19*, S34–39.
(2) Cooper, M. A. *Nat. Rev. Drug Discovery* **2002**, *1*, 515–528.
(3) Nicholson, R. L.; Welch, M.; Ladlow, M.; Spring, D. R. *ACS Chem. Biol.* **2007**, *2*, 24–30.
(4) van den Heuvel, M. G.; Dekker, C. *Science* **2007**, *317*, 333–336.
(5) Hinterdorfer, P.; Dufrene, Y. F. *Nat. Methods* **2006**, *3*, 347–355.
(6) Christman, K. L.; Requa, M. V.; Enriquez-Rios, V. D.; Ward, S. C.; Bradley, K. A.; Turner, K. L.; Maynard, H. D. *Langmuir* **2006**, *22*, 7444–7450.
(7) Hyun, J.; Zhu, Y. J.; Liebmann-Vinson, A.; Beebe, T. P.; Chilkoti, A. *Langmuir* **2001**, *17*, 6358–6367.
(8) Jonkheijm, P.; Weinrich, D.; Kohn, M.; Engelkamp, H.; Christianen, P. C.; Kuhlmann, J.; Maan, J. C.; Nusse, D.; Schroeder, H.; Wacker, R.; Breinbauer, R.; Niemeyer, C. M.; Waldmann, H. *Angew. Chem., Int. Ed. Engl.* **2008**, *47*, 4421–4424.
(9) Alonso, J. M.; Reichel, A.; Piehler, J.; Campo, A. D. *Langmuir* **2008**, *24*, 448–457.
(10) Tinazli, A.; Tang, J.; Valiokas, R.; Picuric, S.; Lata, S.; Piehler, J.; Liedberg, B.; Tampe, R. *Chemistry* **2005**, *11*, 5249–5259.
(11) Klenkar, G.; Valiokas, R.; Lundström, I.; Tinazli, A.; Tampé, R.; Piehler, J.; Liedberg, B. *Anal. Chem.* **2006**, *78*, 3643–3650.
(12) Valiokas, R.; Klenkar, G.; Tinazli, A.; Tampé, R.; Liedberg, B.; Piehler, J. *ChemBiochem* **2006**, *7*, 1325–1329.
(13) Rakickas, T.; Gavutis, M.; Reichel, A.; Piehler, J.; Liedberg, B.; Valiokas, R. *Nano Lett* **2008**, *8*, 3369–3375.
(14) Bhagawati, M.; Ghosh, S.; Reichel, A.; Froehner, K.; Surrey, T.; Piehler, J. *Angew. Chem., Int. Ed. Engl.* **2009**, *48*, 9188–9191.
(15) Camarero, J. A.; Kwon, Y.; Coleman, M. A. *J. Am. Chem. Soc.* **2004**, *126*, 14730–14731.
(16) Kalia, J.; Abbott, N. L.; Raines, R. T. *Bioconjugate Chem.* **2007**, *18*, 1064–1069.
(17) Jean-François, Lutz. *Angew. Chem., Int. Ed.* **2007**, *46*, 1018–1025.
(18) Johnsson, N.; Johnsson, K. *ACS Chem. Biol.* **2007**, *2*, 31–38.
(19) Johnsson, N.; George, N.; Johnsson, K. *Chembiochem* **2005**, *6*, 47–52.
(20) Juillerat, A.; Gronemeyer, T.; Keppler, A.; Gendreizig, S.; Pick, H.; Vogel, H.; Johnsson, K. *Chem. Biol.* **2003**, *10*, 313–317.
(21) Sielaff, I.; Arnold, A.; Godin, G.; Tugulu, S.; Klok, H. A.; Johnsson, K. *Chembiochem* **2006**, *7*, 194–202.
(22) Tugulu, S.; Arnold, A.; Sielaff, I.; Johnsson, K.; Klok, H. A. *Biomacromolecules* **2005**, *6*, 1602–1607.
(23) Yin, J.; Liu, F.; Li, X.; Walsh, C. T. *J. Am. Chem. Soc.* **2004**, *126*, 7754–7755.
(24) Yin, J.; Lin, A. J.; Buckett, P. D.; Wessling-Resnick, M.; Golan, D. E.; Walsh, C. T. *Chem. Biol.* **2005**, *12*, 999–1006.

10.1021/ac902608a
Published on Web 01/21/2010

are highly specific and can be efficiently performed without prior purification of the protein of interest, allowing for capturing proteins from crude lysates to CoA functionalized surfaces.[26] Moreover, several short peptide substrates have been identified, making this approach highly attractive for use with recombinant proteins. These include the ybbR peptide derived from the *B. subtilis* ybbR ORF by phage display[27] and the S6-peptide, which was obtained as a highly efficient substrate for the recognition by the PPTase Sfp.[28]

Here, we have explored PPT-based functional immobilization of proteins fused to the short peptides ybbR and S6 onto glass type surfaces in a flow-through format. To this end, CoA was coupled to a dense poly(ethylene glycol) (PEG) polymer brush, and protein immobilization was monitored in real time by label-free detection using reflectance interference spectroscopy (RIfS). This technique detects protein binding to a thin silica layer on a glass substrate as a shift of the interference spectrum.[29] Immobilization of the extracellular domains of the type I interferon receptor subunits IFNAR1 and IFNAR2 (IFNAR1-EC and IFNAR2-EC, respectively) fused to ybbR- and S6-tags mediated by the PPTase Sfp was investigated. The functionality of the immobilized protein was probed quantitatively by monitoring binding of the protein ligand interferon-α2 (IFNα2). We explored immobilization at different termini, as well as immobilization of ybbR-tagged IFNα2. Moreover, we established protein micropatterning based on PPT-specific immobilization using photochemical deprotection of caged amine groups on the surface, and we demonstrate specific protein−protein interactions in these micropatterns.

EXPERIMENTAL SECTION

Materials. Homofunctional diamino-poly(ethylene glycol) (DAPEG) with an average molecular mass of 2000 g/mol was purchased from Rapp Polymere, Tübingen, Germany. 2-Mercaptoethanol, manganese(II) chloride tetrahydrate, HEPES, and sodium chloride were purchased from Carl Roth, Karlsruhe, Germany. Oregon Green 488 maleimide was purchased from Invitrogen. Streptavidin labeled with ATTO 565 (^{AT565}SAv) was purchased from ATTO-TEC GmbH, Siegen, Germany. A 75 W xenon lamp fitted with a 280−400 nm dichroic mirror was purchased from Newport Spectra-Physics and microstructured masks for photopatterning (chrome on quartz) were obtained from NB Technologies, Bremen, Germany. CoA-488 and phosphopantetheinyl transferase Sfp were purchased from Covalys Biosciences, Witterswil, Switzerland. All other chemicals were purchased from Sigma−Aldrich.

Protein Production, Purification, and Labeling. IFNα2, IFNα2-YNS, and IFNAR2-EC carrying an N-terminal ybbR-tag (ybbR-IFNα2, ybbR-IFNα2-YNS, and ybbR-IFNAR2) were cloned by insertion of an oligonucleotide linker coding for the ybbR peptide (DSLEFIASKLA) into the *Nde*I restriction site upstream of the corresponding genes in the plasmids pT72Cα2 and pT72CR2, respectively.[30] The proteins were expressed and purified by the same protocols established for wild-type IFNα2 and wild-type IFNAR2-EC.[31] IFNAR2 with C-terminal ybbR- and S6-tags (IFNAR2-ybbR and IFNAR2-S6) were cloned by inserting the corresponding oligonucleotide linker coding for the corresponding peptides sequences (GDSLSWLLRLLN in case of S6) into a *Sal*I restriction site, which was generated at the C-terminus of IFNAR2-EC in pT72CR2 by removing the stop codon by site-directed mutagenesis. These proteins were expressed in *E. coli*, refolded from inclusion bodies, and purified as described previously.[30,32] IFNAR2-ybbR and ybbR-IFNα2 were labeled by PPT using CoA-488 and Sfp according to published protocols.[33] His-tagged IFNAR1-EC and its mutant N23C were expressed in *Sf*9 insect cells and purified by IMAC as described previously.[34] IFNAR1-EC N23C was site-specifically labeled with Oregon Green 488 (^{OG488}IFNAR1-EC) as described recently.[35] His-tagged IFNAR1-EC was fused to a C-terminal ybbR-tag by insertion of an oligonucleotide linker coding for the ybbR peptide and was expressed and purified the same way as IFNAR1-EC.

Surface Chemistry. Surface chemistry was carried out on transducer slides for RIfS detection (a thin silica layer on a glass substrate)[36] as well as standard glass cover slides for fluorescence microscopy. Surface coating with a thin PEG polymer brush and further functionalization with maleimide groups was carried out as described in detail previously:[37] After surface cleaning in fresh Piranha solution (one part 30% H_2O_2 and two parts concentrated H_2SO_4; caution, highly corrosive), the surface was activated by reaction with pure (3-glycidyloxypropyl)trimethoxysilane for 1 h at 75 °C. Subsequently, the surface was reacted with molten DAPEG for 4 h at 75 °C. For functionalization with maleimide groups, the amine-functionalized surfaces were incubated under a saturated solution of 3-(maleimido)propionic acid *N*-hydroxysuccinimide ester (MPA-NHS) in dry DMF for 30 min at room temperature. All further steps were carried out in situ under aqueous conditions in a flow-through format (see below).

Surface Patterning. Photolithographic patterning was performed using nitroveratryloxycarbonyl (Nvoc) chloride as a photocleavable amine protecting group. For caging of the surface amine groups, DAPEG-functionalized surfaces were incubated with a saturated solution of Nvoc chloride in chloroform for 1 h at 75 °C. Uncaging of the amine groups was achieved by irradiation through a photomask for 5 min using a 75 W xenon lamp equipped with a 280−400 nm dichroic mirror. Irradiation was carried out in the presence of 50 mM semicarbazide in methanol in order to minimize side reactions. Subsequently, deprotected amine groups were reacted with biotinamidohexanoic acid *N*-hydroxysuccinimide ester (biotin-NHS). For binary patterning, the surface was

(25) George, N.; Pick, H.; Vogel, H.; Johnsson, N.; Johnsson, K. *J. Am. Chem. Soc.* **2004**, *126*, 8896–8897.
(26) Wong, L. S.; Thirlway, J.; Micklefield, J. *J. Am. Chem. Soc.* **2008**, *130*, 12456–12464.
(27) Yin, J.; Straight, P. D.; McLoughlin, S. M.; Zhou, Z.; Lin, A. J.; Golan, D. E.; Kelleher, N. L.; Kolter, R.; Walsh, C. T. *Proc. Natl. Acad. Sci. U.S.A.* **2005**, *102*, 15815–15820.
(28) Zhou, Z.; Cironi, P.; Lin, A. J.; Xu, Y.; Hrvatin, S.; Golan, D. E.; Silver, P. A.; Walsh, C. T.; Yin, J. *ACS Chem. Biol.* **2007**, *2*, 337–346.
(29) Brecht, A.; Gauglitz, G.; Polster, J. *Biosens. Bioelectron.* **1993**, *8*, 387–392.
(30) Piehler, J.; Schreiber, G. *J. Mol. Biol.* **1999**, *289*, 57–67.
(31) Piehler, J.; Roisman, L. C.; Schreiber, G. *J. Biol. Chem.* **2000**, *275*, 40425–40433.
(32) Piehler, J.; Schreiber, G. *J. Mol. Biol.* **1999**, *294*, 223–237.
(33) Yin, J.; Lin, A. J.; Golan, D. E.; Walsh, C. T. *Nat. Protoc.* **2006**, *1*, 280–285.
(34) Lamken, P.; Lata, S.; Gavutis, M.; Piehler, J. *J. Mol. Biol.* **2004**, *341*, 303–318.
(35) Strunk, J. J.; Gregor, I.; Becker, Y.; Li, Z.; Gavutis, M.; Jaks, E.; Lamken, P.; Walz, T.; Enderlein, J.; Piehler, J. *J. Mol. Biol.* **2008**, *377*, 725–739.
(36) Schmitt, H. M.; Brecht, A.; Piehler, J.; Gauglitz, G. *Biosens. Bioelectron.* **1997**, *12*, 809–816.
(37) Piehler, J.; Brecht, A.; Valiokas, R.; Liedberg, B.; Gauglitz, G. *Biosens. Bioelectron.* **2000**, *15*, 473–481.

again irradiated as before but without a photomask. This led to the deprotection of the remaining surface amines which were subsequently reacted with MPA-NHS.

Binding Assays. Protein immobilization and protein interactions were monitored by RIfS and by total internal reflection fluorescence spectroscopy (TIRFS). Label-free detection by RIfS is based on probing changes in optical thickness of a thin silica layer by white light interference.[29] Changes in the surface loading upon protein binding and dissociation are detected in real time as a shift of the interference spectrum on the wavelength axis. A change in surface loading by 1 pg/mm^2 leads to a shift of the interference minimum (1.5th order) by 1.2 pm as determined by calibration experiments with radioactively labeled proteins.[38] The measurements were performed under continuous flow-through conditions using a home-built setup as described in detail earlier.[36,39] TIRFS is based on selective fluorescence excitation at the substrate surface by an evanescent field. A home-built TIRFS setup with simultaneous reflectance interference detection as described previously[40,41] was used for detection of interactions with fluorescence-labeled proteins. Maleimide-functionalized RIfS transducer slides (prepared as described above) were equilibrated in HBS (20 mM HEPES pH 7.5, 150 mM sodium-chloride and 0.01% Triton X-100) and then reacted with 1 mM CoA in HBS. Prior to protein immobilization, the remaining maleimide groups were blocked by injection of 10 mM 2-mercaptoethanol in HBS. Subsequently, 1 μM of ybbR-IFNAR2 in HBS was immobilized in the presence of 1 μM Sfp and 10 mM Mn^{2+} ions. Surface-bound metal ions were removed by an injection of 25 mM EDTA. Then, the activity of the immobilized protein was probed by injecting a suitable binding partner: ybbR-IFNAR2, IFNAR2-ybbR, and IFNAR2-S6 were probed by injection of the ligand IFNα2. YbbR-IFNα2, and ybbR-IFNα2-YNS were probed by injection of IFNAR2-EC and IFNAR1-EC, respectively.

Association and dissociation curves were fitted using the BIAevaluation 3.1 software (GE Healthcare). Standard kinetic models assuming a 1:1 Langmuir interaction as provided by the software were applied. For binding kinetics at relatively high protein surface concentrations employed in RIfS experiments, simultaneous fitting of the association and dissociation curves by a model considering mass transport effects was applied. At low protein surface concentrations used in TIRFS experiments, association and dissociation curves were fitted separately with single exponential functions assuming an unbiased 1:1 Langmuir interaction.

Fluorescence Imaging. Micropatterns of fluorescence-labeled proteins were imaged by means of a confocal laser-scanning microscope (FluoView 1000, Olympus). A 40 mW multiline argon ion laser was used for the excitation of AT488 and a 20 mW 559 nm diode laser for the excitation of ATTO 565. All experiments were carried out using a home-built flow cell, and ybbR-IFNAR2 was immobilized on patterned cover slides under the same conditions as described in the previous section. In order to confirm the activity of the immobilized ybbR-IFNAR2, 100 nM fluorescence labeled IFNα2 (^{AT488}IFNα2) was injected. The specificity of the interaction was verified by competition with unlabeled IFNα2. Binary patterns were developed by the injection of 100 nM ^{AT565}SAv, which was captured by the patterned biotin on the surface. Dual color images were obtained by sequential line scanning in order to minimize cross-talk between the two channels.

RESULTS AND DISCUSSION

Specific and Functional Protein Immobilization by PPT. In order to immobilize and pattern proteins onto CoA-functionalized glass-type surfaces through direct PPT, we implemented a bottom-up approach for modification of glass-type surfaces as outlined in Scheme 1. This approach is based on a previously published methodology for obtaining a dense PEG polymer brush functionalized with amine groups, which renders glass-type surfaces highly biocompatible.[37] For direct attachment of CoA, the surface amine groups were converted into maleimide groups by reaction with a heterobifunctional cross-linker MPA-NHS. Binding of CoA to these surfaces followed by PPT-mediated immobilization of proteins was probed in real time by RIfS detection. A typical binding experiment is schematically depicted in Figure 1a, and the corresponding RIfS trace is shown in Figure 1b: in the first step, 1 mM CoA was injected, leading to a rapid shift of the interference spectrum of ~500 pm due to the reaction with surface maleimide groups. This signal corresponds to a surface concentration of ~420 pg/mm^2 or ~0.57 pmol/mm^2 CoA yielded by this reaction. This is in line with the surface concentration of PEG chains on the surface (1.6 pmol/mm^2),[37] which limits the maximum number of maleimide moieties on the surface. The remaining maleimide groups were quenched by reaction with 2-mercaptoethanol in order to avoid immobilization of Sfp through its exposed cysteine residues (cf. Supporting Information Figure S-1). During injection of Sfp and ybbR-IFNAR2 in presence of Mn^{2+} ions (cf. Supporting Information Figure S-2), a strong increase of the signal was observed, which decayed rapidly during rinsing with buffer. This signal is mainly due to Sfp interacting with CoA on the surface, since no signal was observed in absence of CoA on the surface (Figure 1b). Upon injection of Sfp and IFNAR2-EC without an ybbR-tag, a small amount of protein (~300 pm) remained stably bound to the surface (Figure 1d). However, similar amounts of protein remained on the surface when only Sfp was injected (data not shown), indicating that the main contribution of this signal was due to residual amounts of Sfp on the surface. An insignificant amount of protein of less than 20 pm was observed in the absence of CoA on the surface (Figure 1b), confirming the very low level of nonspecific binding to the PEG polymer brush. When Sfp was injected in presence of ybbR-IFNAR2, ~1 nm protein was stably immobilized on the surface. Thus, a net amount of ~700 pm (~0.58 ng/mm^2, 23 fmol/mm^2) ybbR-IFNAR2 was immobilized under these conditions. This surface concentration of ybbR-IFNAR2 corresponds to ~15% of a protein monolayer, assuming a surface area of 10 nm^2 per protein molecule. Subsequent injection of the ligand IFNα2 confirmed functional immobilization of ybbR-IFNAR2: fast binding of IFNα2 was observed during injection and dissociation during rinsing (Figure 1e). Without CoA on the surface or with nontagged IFNAR2-EC during the injection of Sfp/Mn^{2+}, no significant binding of IFNα2 was

(38) Hanel, C.; Gauglitz, G. *Anal. Bioanal. Chem.* **2002**, *372*, 91–100.
(39) Piehler, J.; Schreiber, G. *Anal. Biochem.* **2001**, *289*, 173–186.
(40) Gavutis, M.; Lata, S.; Lamken, P.; Müller, P.; Piehler, J. *Biophys. J.* **2005**, *88*, 4289–4302.
(41) Gavutis, M.; Lata, S.; Piehler, J. *Nat. Protoc.* **2006**, *1*, 2091–2103.

Scheme 1. Surface Chemistries[a]

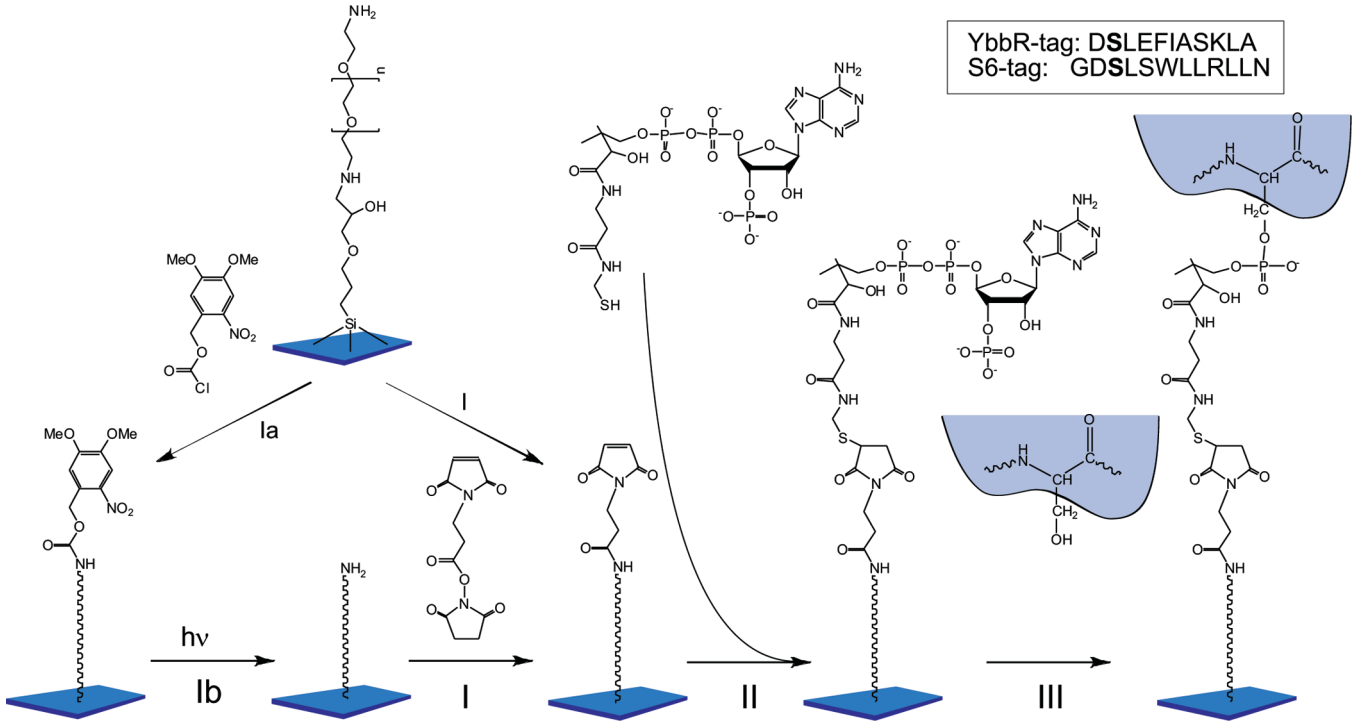

[a] After coupling of a PEG polymer brush, terminal amine groups were reacted with MPA-NHS (I) followed by coupling of CoA (II) and protein immobilization via Sfp-catalyzed PPT (III) through the serine residue on the corresponding tag (marked in bold in the sequences of the ybbR- and the S6-tag). The last two steps were carried out in situ with the transducer mounted in the flow system. For surface patterning, terminal amine groups of the PEG polymer brush were reacted with Nvoc-chloride (Ia) and subsequently UV-illuminated through a mask to generate free amine groups (Ib) in selected areas. These were further functionalized with MPA-NHS and CoA by the reactions I and II followed by PPT-mediated protein immobilization.

observed (Figure 1e), confirming the high specificity of the PPT-mediated immobilization. Moreover, no binding of IFNα2 was observed in presence of soluble IFNAR2-EC, corroborating the specificity of the interaction (Supporting Information Figure S-3). Fitting of the binding curve by a kinetic model considering mass transport limitations, rate constants of 1×10^6 M^{-1} s^{-1} for association, and 0.02 s^{-1} for dissociation were obtained (Figure 1f). These values are in excellent agreement with previously published rate constants obtained for IFNAR2-EC immobilized by site-specific attachment through antibodies or His-tag.[35,39,42] The binding amplitude of 400 pm observed for IFNα2 binding indicates that ~70% of the immobilized ybbR-IFNAR2 on the surface was active, taking the molecular masses of 20 kDa for IFNα2 and 25 kDa for IFNAR2-EC into account. Similar activities have been observed for site-directed immobilization of IFNAR2-EC through a His-tag,[10,43] while no binding activity was obtained for nonspecifically adsorbed IFNAR2-EC and much faster dissociation was observed upon amine-specific immobilization.[39] These results therefore demonstrate that PPT-mediated immobilization maintains the activity of the immobilized protein.

Generic Application of PPT-Based Immobilization. In order to further explore the capabilities for functional protein immobilization through the ybbR-tag, we tested immobilization of IFNα2 with an N-terminal ybbR-tag (ybbR-IFNα2). Both ybbR-IFNα2 wildtype and ybbR-IFNα2-YNS were readily immobilized on CoA-functionalized surfaces under the same conditions as shown for ybbR-IFNAR2 (data not shown). A net amount of typically 0.3−0.5 ng/mm^2 protein was immobilized by this procedure (data not shown). Reversible binding of IFNAR2-EC to both ybbR-IFNα2 (Supporting Information Figure S-4) and ybbR-IFNα2-YNS (Figure 2a) was observed, confirming functional immobilization of these proteins. Binding specificity was confirmed by a binding inhibition assay with free IFNα2 in solution, reducing binding of IFNAR2-EC close to the background signal (data not shown). Strikingly, nearly unchanged levels of IFNAR2-EC binding were obtained 24 h after immobilization of ybbR-IFNα2 (Supporting Information Figure S-5), highlighting the highly biocompatible immobilization conditions. For immobilized ybbR-IFNα2-YNS, which has a much higher binding affinity toward IFNAR1 than IFNα2,[44] specific binding of IFNAR1-EC to immobilized ybbR-IFNα2-YNS was observed (Figure 2b) confirming functional protein immobilization. For probing simultaneous binding of both IFNAR1-EC and IFNAR2-EC, we employed TIRFS using similar flow-through conditions as in the RIfS experiments. Binding of fluorescence-labeled IFNAR1-EC (^{OG488}IFNAR1-EC) was selectively detected by TIRFS (Figure 2c). For probing ternary complex formation, dissociation of ^{OG488}IFNAR1-EC in presence and in absence of unlabeled IFNAR2-EC was measured. A significant change in the dissociation kinetics indicated that immobilized ybbR-IFNα2-YNS can simultaneously interact with IFNAR1-EC and IFNAR2-EC in a slightly cooperative manner (Figure 2d).

Comparison of N- and C-Terminal Fusion of the Peptide Tags. In order to further explore generic application of PPT-mediated protein immobilization, we fused the ybbR-tag to the

(42) Lamken, P.; Gavutis, M.; Peters, I.; Van der Heyden, J.; Uze, G.; Piehler, J. *J. Mol. Biol.* **2005**, *350*, 476–488.
(43) Lata, S.; Piehler, J. *Anal. Chem.* **2005**, *77*, 1096–1105.
(44) Kalie, E.; Jaitin, D. A.; Abramovich, R.; Schreiber, G. *J. Biol. Chem.* **2007**, *282*, 11602–11611.

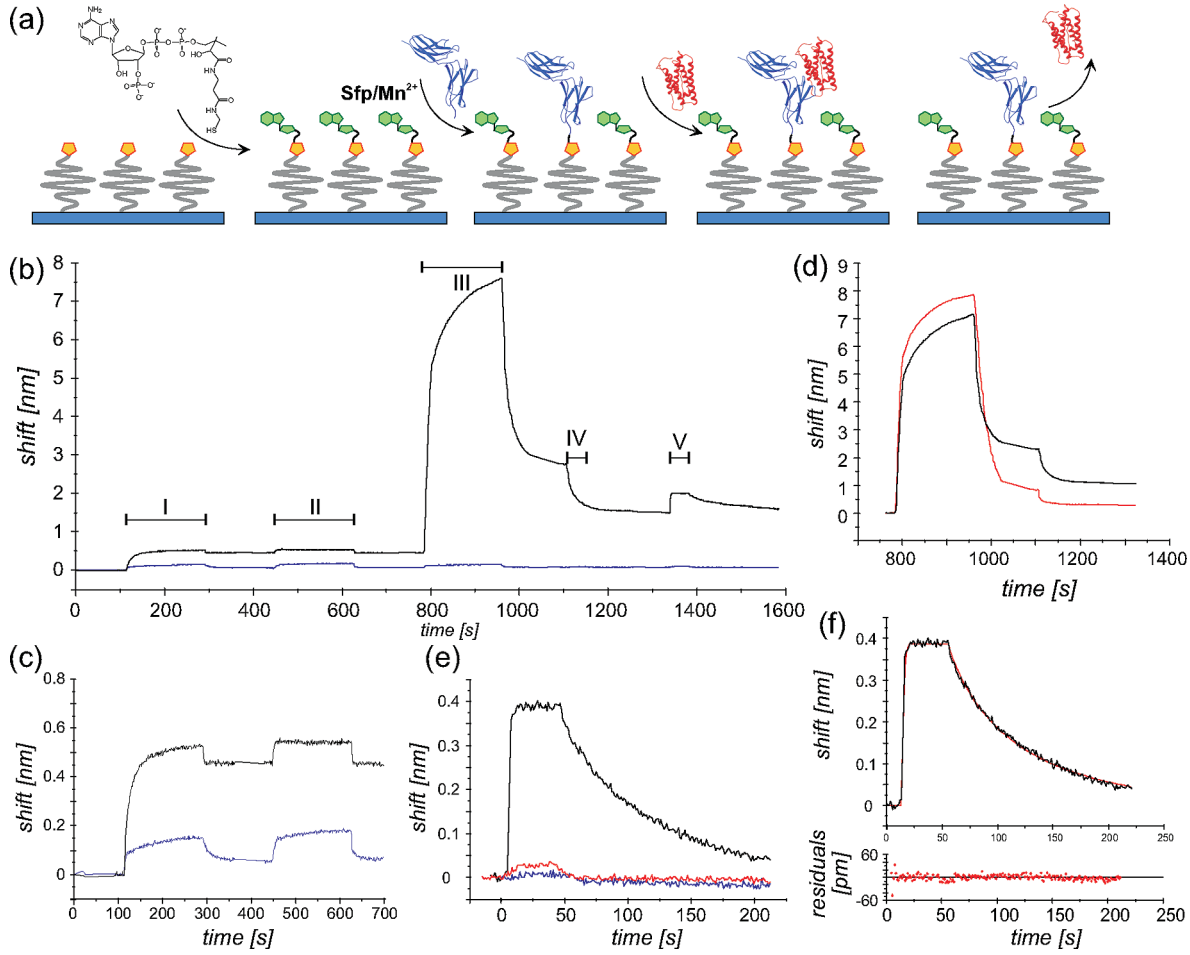

Figure 1. Immobilization of ybbR-IFNAR2 onto modified glass-type surfaces as monitored by RIfS. (a) Schematic of the key reaction steps and binding reactions performed in the flow cell and (b) a typical RIfS trace for this experiment (black line): After coupling of CoA (1 mM) to a maleimide-functionalized surface (I), the remaining maleimide groups were blocked by injection of 10 mM 2-mercaptoethanol (II). Subsequently, Sfp (1 μM) mixed with ybbR-IFNAR2 (1 μM) in buffer containing 10 mM Mn^{2+} was injected (III), followed by a rinse with 25 mM EDTA (IV) and the injection of 1 μM IFNα2 (V). As a control, the same sequence of injections is shown, where 2-mercaptoethanol instead of CoA was injected during the first injection (blue). (c) A magnified overlay of the signals during injection of CoA and 2-mercaptoethanol (black) compared to two sequential injections of 2-mercaptoethanol used as a control (blue). (d) Overlay of the signals during injection of Sfp/Mn^{2+} in presence of ybbR-IFNAR2 (black) or IFNAR2-EC (red), followed by rinsing and washing with EDTA. (e) Comparison of the IFNα2 binding signal obtained for ybbR-IFNAR2 immobilized with (black) and without (red) CoA on the surface, and for a control of specificity using IFNAR2-EC without a PPT-tag (blue). (f) Association and dissociation kinetics of IFNα2 fitted using a kinetic model considering mass transport limitations.

C-termini of IFNAR1-EC (IFNAR1-ybbR) and IFNAR2-EC (IFNAR2-ybbR). Upon immobilization of these proteins under the same conditions described above, only very low net amounts of proteins were stably bound on the surface, and binding of the ligand IFNα2 to IFNAR2-ybbR and IFNα2-YNS to IFNAR1-ybbR was not detectable by RIfS. Upon more sensitive detection by TIRFS, however, specific binding of IFNα2 and IFNα2-YNS, which were site-specifically labeled with ATTO488 (^{AT488}IFNα2 and ^{AT488}IFNα2-YNS, respectively), was revealed (Figure 3a,b). The binding constants obtained by fitting of a model assuming unbiased 1:1 interaction were in good agreement with the published rate constants, confirming functional immobilization of these proteins on the surface, albeit at very low levels. Labeling of IFNAR1-ybbR and IFNAR2-ybbR with CoA-488 by PPT yielded labeling degrees >50%, confirming the integrity of the corresponding ybbR-tags (data not shown). Thus, immobilization of proteins with C-terminal ybbR-tags appears to be much less efficient than N-terminal ybbR-tags. A possible reason could be that the amino acids adjacent to the ybbR-tag are important for PPT efficiencies.

In order to overcome this limitation, we tested the S6-tag, an alternative peptide tag for PPT. This 12 amino acid tag was developed for orthogonal protein labeling by different PPTases and has a ~2-fold higher k_{cat}/K_m for PPT by Sfp compared to the ybbR-tag.[28] Strikingly, efficient immobilization of IFNAR2-EC fused to a C-terminal S6 tag was observed (Figure 3c). Both the immobilization level of IFNAR2-S6 as well as the binding amplitude observed upon injection of IFNα2 were significantly higher compared to those obtained for IFNAR2-ybbR. However, approximately 50% of the immobilization level observed for ybbR-IFNAR2-EC was obtained (Figure 3d). Such immense differences between these tags for PPT and such differences for these tags being fused to N- and C-termini are not in line with the properties observed for labeling experiments with these tags described in literature.[28,33] A potentially important difference between these tags is the additional glycine residue upstream of the shared Asp-Ser-Leu motif containing the serine residue, to which the phosphopantetheinyl moiety is transferred. To our knowledge, the importance of this residue has not been systematically explored.

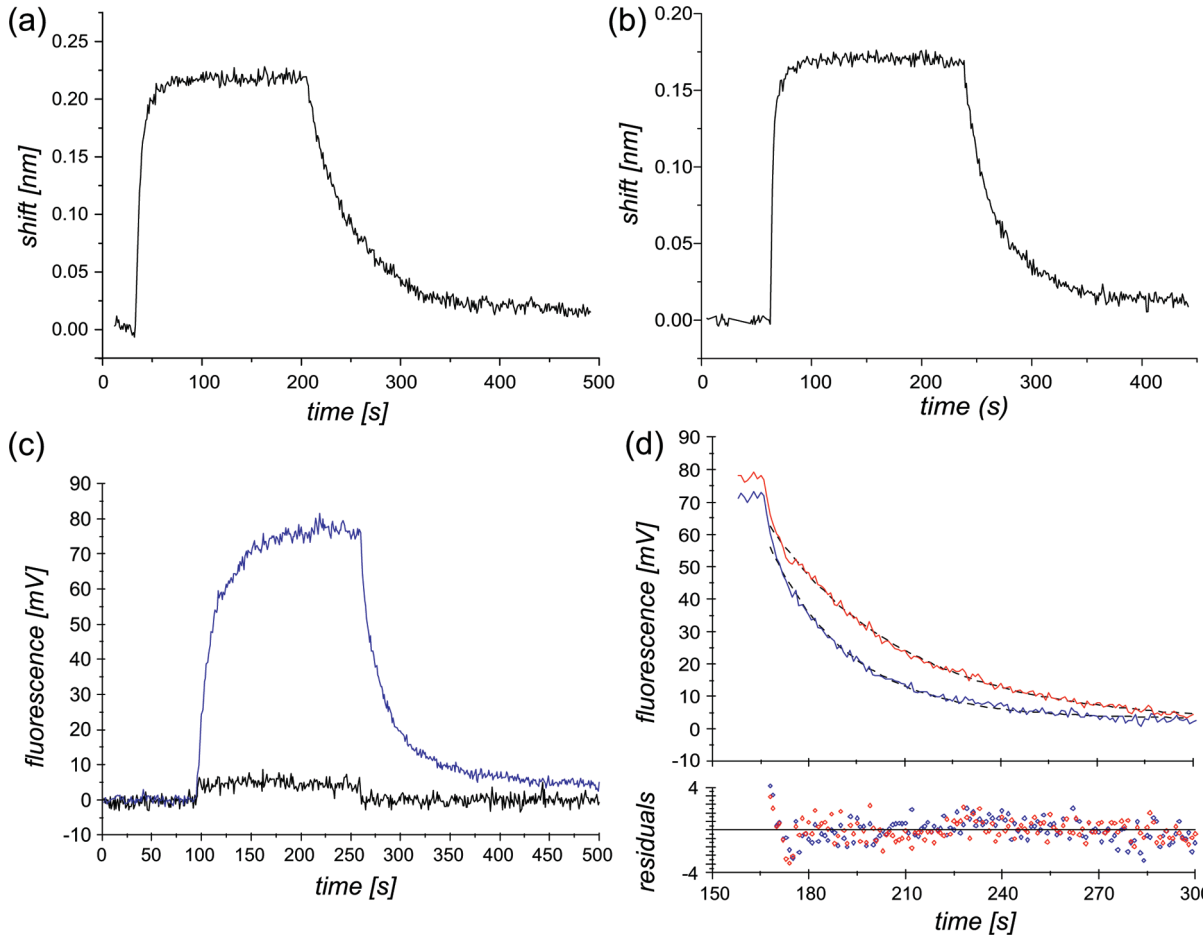

Figure 2. Real-time protein interaction experiments with ybbR-tagged IFNα2 immobilized by PPT. (a) 1 μM IFNAR2 binding to immobilized ybbR-IFNα2-YNS as detected by RIfS. (b) 1 μM IFNAR1-EC binding to immobilized ybbR-IFNα2-YNS as detected by RIfS. (c) 100 nM ^{OG488}IFNAR1-EC binding to immobilized ybbR-IFNα2-YNS as detected by TIRFS (blue). As a control, binding of 100 nM ^{OG488}IFNAR1-EC to surfaces prior to the immobilization of ybbR-IFNα2-YNS is shown (black). (d) Comparison of the dissociation kinetics of ^{OG488}IFNAR1-EC bound to immobilized ybbR-IFNα2-YNS in absence (blue) and in presence (red) of unlabeled IFNAR2-EC.

In case of the proteins used in this study, Thr and Phe were located upstream of the ybbR-tag in case of IFNAR2-ybbR and IFNAR1-ybbR, respectively, compared to a Met residue for the N-terminal ybbR-tags. Further systematic studies are required to resolve this issue.

Functional Protein Patterning by PPT. With this powerful immobilization method in hand, we aimed for extending this approach toward lateral organization of proteins on surfaces in micrometer dimensions. Photodeprotection of caged amine functionalities has been demonstrated to be a versatile approach toward biofunctional surface patterning.[9,45−47] On the basis of this approach, we implemented PPT-based functional surface patterning by caging of surface amine groups with Nvoc chloride after coupling of the diamino-PEG as depicted in Scheme 1 (step Ia). In the first step, the caging reaction on the surface and the uncaging by UV irradiation was analyzed by reacting free surface amines with biotin-NHS. The amount of immobilized biotin molecules was probed by streptavidin binding using RIfS (Figure 4a). Very low streptavidin binding compared to the positive control confirmed efficient protection of surface amines by reaction with Nvoc chloride (Figure 4a). Upon UV-irradiation in presence of 50 mM semicarbazide, ~75% recovery of streptavidin binding was observed, confirming successful uncaging of surface amines. The same approach was used for coupling MPA-NHS, followed by reaction with CoA and subsequent PPT-mediated immobilization of ybbR-IFNAR2. The amount of ybbR-IFNAR2 on the surface was quantified by probing the binding of IFNα2 using RIfS (Figure 4b). Only insignificant binding of IFNα2 was detected after caging the surface amines with Nvoc chloride prior to the reaction with MPA-NHS, confirming the specificity of the immobilization procedure. Upon uncaging surface amines, strong binding of IFNα2 was observed, reaching ~75% of the binding amplitude obtained for the positive control.

With this efficient protocol in hand we explored photolithographic protein patterning. In order to generate binary protein patterns, we followed a two-step illumination scheme (Figure 5a): After UV-illumination through a photomask, the uncaged amine groups were reacted with biotin-NHS, followed by another exposure to UV light without a photomask and coupling of MPA-NHS. The coverslide was then mounted in a flow cell and functionalized with CoA under flow-through conditions followed by coupling of ybbR-IFNAR2 in presence of Sfp. Upon injection of ^{AT488}IFNα2, patterns of green fluorescence were observed

(45) Jonas, U.; del Campo, A.; Kruger, C.; Glasser, G.; Boos, D. *Proc. Natl. Acad. Sci. U.S.A.* **2002**, *99*, 5034–5039.
(46) Stegmaier, P.; del Campo, A. *Chemphyschem* **2009**, *10*, 357–369.
(47) Chen, S.; Smith, L. M. *Langmuir* **2009**, *25*, 12275–12282.

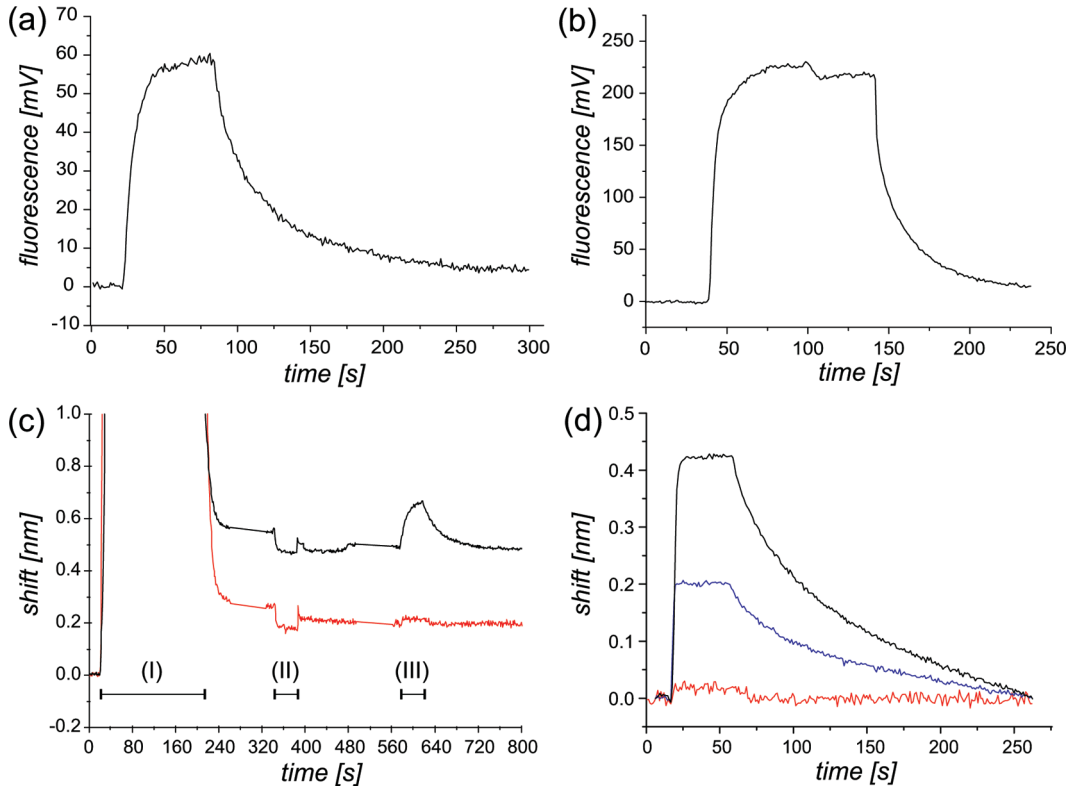

Figure 3. Immobilization of IFNAR2-EC and IFNAR1-EC through C-terminal S6 and ybbR-tags. (a) Binding of 100 nM ^{AT488}IFNα2 to immobilized IFNAR2-ybbR as detected by TIRFS. (b) Binding of 100 nM ^{AT488}IFNα2-YNS to immobilized IFNAR1-ybbR as detected by TIRFS. (c) Immobilization of IFNAR2-S6 by PPT (black) compared to the immobilization of IFNAR2-ybbR (red). Only the injection of Sfp (I), EDTA (II), and IFNα2 are shown. (d) Binding signals of 1 μM IFNα2 to immobilized IFNAR2-S6 (blue), IFNAR2-ybbR (red), and ybbR-IFNAR2 (black) in comparison.

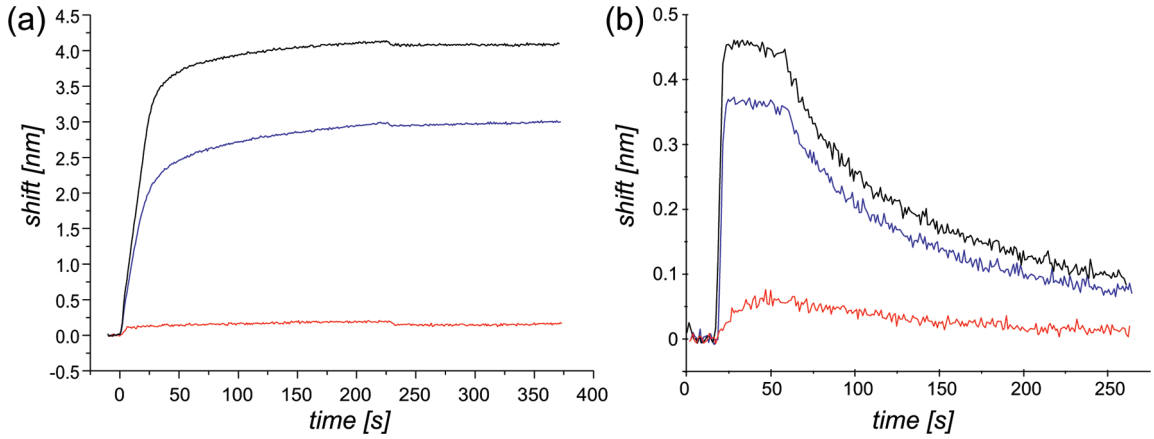

Figure 4. Caging of surface amines by Nvoc chloride probed by protein binding experiments using RIfS. (a) Binding of 100 nM streptavidin to surfaces reacted with biotin-NHS before (black) and after (red) caging with Nvoc chloride, and after UV-illumination of Nvoc-caged amines (blue). (b) Binding of 1 μM IFNα2 to ybbR-IFNAR2 immobilized by PPT after caging (red) and after uncaging (blue) of surface amines. For comparison, a positive control without caging the amine groups is shown (black).

in the areas which were not illuminated during the first illumination cycle, indicating successful immobilization of ybbR-IFNAR2 into the micropatterns (Figure 5b). IFNα2 binding proved reversible and complete washout in presence of unlabeled IFNα2 was obtained. Moreover, no binding of ^{AT488}IFNα2 was detectable when incubated in presence of unlabeled IFNα2, confirming binding specificity. In the next step, we tested binding of orange-fluorescent streptavidin ^{AT565}SAv to the surface. Specific targeting of ^{AT565}SAv to the grid, which was UV-illuminated prior to biotin-NHS coupling, was observed (Figure 5c), confirming successful binary protein patterning. Upon addition of unlabeled IFNα2, selective washout of ^{AT488}IFNα2, but not ^{AT565}SAv, was observed, confirming highly specific binary protein targeting into microstructures.

CONCLUSIONS

Site-specific covalent immobilization and lateral organization of recombinant proteins on planar substrates is highly demanded for numerous analytical and biotechnological applications. Generic approaches providing highly functional protein microstructures

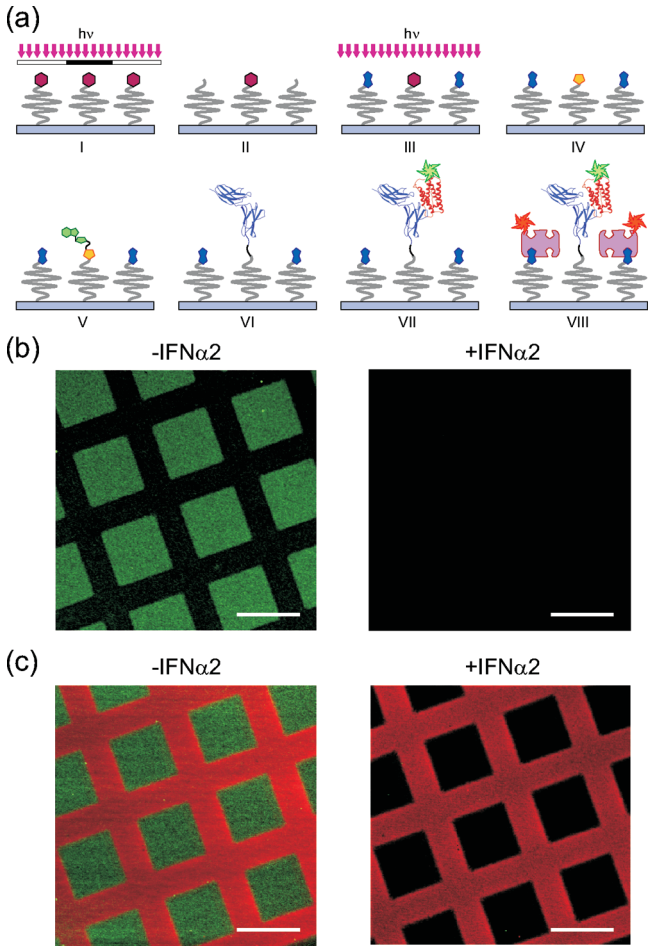

Figure 5. Functional patterning by PPT-mediated immobilization. (a) Schematic of the surface chemistry (top) and further modification in the flow cell (bottom). Nvoc-caged surfaces were first UV-deprotected through a photomask (I), and the deprotected areas (II) were functionalized with biotin-NHS, followed by uncaging of the remaining amines with UV light (III). Subsequently, the uncaged amines were functionalized with MPA-NHS (IV). After the coverslide was mounted into the flow cell, surfaces were first reacted with CoA (V) followed by PPT-mediated immobilization of ybbR-IFNAR2 (VI). Subsequently, protein binding assays with ^{AT488}IFNα2 (VII) and ^{AT565}SAv (VIII) were carried out. (b) CLSM images after binding of ^{AT488}IFNα2 to immobilized ybbR-IFNAR2 in absence (left) and in presence (right) of unlabeled IFNα2. (c) Dual color CLSM images after sequential incubation with 100 nM ^{AT488}IFNα2 and 100 nM ^{AT565}SAv (left), and after exchanging ^{AT488}IFNα2 by 1 μM unlabeled IFNα2 (right). All scale bars represent 20 μm.

are required. Compared to other biochemical and enzymatic immobilization methods, PPT offers the advantage of relatively rugged coupling protocols and compatibility with nearly all proteins. Moreover, highly specific PPT to short peptide tags fused on N- or C-termini of proteins is possible. While enzymatic PPT has already been successfully employed for immobilization of model proteins on solid support,[26] quantitative assessment of immobilization efficiencies and protein functionality has not yet been reported. Advanced bioanalytical and biophysical techniques, however, require highly efficient functional protein immobilization on solid supports. Here, we have quantitatively explored site-specific, covalent immobilization by enzymatic PPT transfer from CoA-functionalized, biocompatible surfaces for generating functional protein micropatterns. Efficient coupling of CoA to a PEG polymer brush surface by a bottom-up surface chemistry was confirmed by label-free detection, indicating a high binding capacity of the surface. Under these conditions, efficient immobilization of proteins with an N-terminal ybbR-tag at moderate concentrations (1 μM) was obtained within relatively short times (150 s), enabling functional characterization of the immobilized proteins by label-free detection. Quantitative protein−protein interactions measurements confirmed that the functional properties of the immobilized proteins were homogeneous and not affected by the immobilization procedure. While C-terminal ybbR-tags were not suitable for efficient immobilization, this problem was overcome by using the S6-tag. Since protein concentration substantially below the K_m values reported for these tags (50−100 μM) have been applied, much faster immobilization will be possible by increasing protein concentrations. We have here implemented a simple bottom-up surface modification approach for glass-type substrates, which enables highly functional protein patterning and opens exciting prospects for applications in combination with fluorescence imaging techniques. The immobilization procedure itself, however, is readily adapted to different substrates and immobilization schemes. This method, therefore, will be a valuable tool for covalent functional protein immobilization in numerous demanding bioanalytical and biophysical applications such as label-free biosensor detection, single molecule force spectroscopy, and fluorescence imaging techniques.

ACKNOWLEDGMENT

We thank Gabriele Hikade and Hella Kenneweg for protein production, Covalys Biosciences for technical support with PPT technology, and NB-Technologies for providing photomasks. This project was supported by funding from the DFG (PI 405-4 and EXC 115) and by the BMBF (0312034). J.P was supported by a Heisenberg Professorship from the DFG (PI 405-3) and S.W. by a Ph.D. fellowship from the Minerva Foundation.

SUPPORTING INFORMATION AVAILABLE

Additional information as noted in the text. This material is available free of charge via the Internet at http://pubs.acs.org.

Received for review November 13, 2009. Accepted December 26, 2009.

AC902608A